Title

A single microRNA miR-195 rescues the arrested B cell development induced by EBF1 deficiency

Authors

Y. Miyatake[1], T. Ikawa[2], R. Yanagiya[1], R. Kotaki[1], K. Kameda[1], R. Koyama-Nasu[3,4], K. Okuyama[5], K. Hirano[6], H. Hosokawa[6], K. Hozumi[6], M. Ohtsuka[7], T. Kishikawa[8], C. Shibata[8], M. Otsuka[9], R. Maruyama[10], K. Ando[11], T. Kurosaki[12,13,14], H. Kawamoto[15], and A. Kotani[1*]

Affiliations

[1] Department of Innovative Medical Science, Tokai University School of Medicine, Isehara, Kanagawa, 259-1193, Japan

[2] Division of Immunology and Allergy, Research Institute for Biomedical Sciences, Tokyo University of Science, Noda, Chiba, 278-0022, Japan

[3] Department of Immunology, Graduate School of Medicine, Chiba University, Chiba, Chiba, 260-0856, Japan

[4] Department of Experimental Immunology, Graduate School of Medicine, Chiba University, Chiba, Chiba, 260-0856, Japan

[5] Laboratory for Transcriptional Regulation, RIKEN Center for Integrative Medical Sciences, Yokohama, Kanagawa, 230-0045, Japan

[6] Department of Immunology, Tokai University School of Medicine, Isehara, Kanagawa, 259-1193, Japan

24 [7] Department of Molecular Life Science, Tokai University School of Medicine,
25 Isehara, Kanagawa, 259-1193, Japan

26 [8] Department of Gastroenterology, Graduate School of Medicine, The University of
27 Tokyo, Bunkyo-ku, Tokyo, 113-0033, Japan

28 [9] Department of Gastroenterology and Hepatology, Okayama University Hospital,
29 Okayama, Okayama, 700-8558, Japan

30 [10] Project for Cancer Epigenomics, Cancer Institute, Japanese Foundation for Cancer
31 Research, Koto-ku, Tokyo, 135-8550, Japan

32 [11] Hematology and Oncology, Research Institute for Radiation Biology and Medicine,
33 Hiroshima University, Hiroshima, Hiroshima, 734-8551, Japan

34 [12] Laboratory of Lymphocyte Differentiation, WPI Immunology Frontier Research
35 Center, Osaka University, Suita, Osaka, 565-0871, Japan

36 [13] Laboratory for Infectious Disease Education and Research, Osaka University,
37 Suita, Osaka, 565-0871, Japan

38 [14] Laboratory for Lymphocyte Differentiation, RIKEN Center for Integrative Medical
39 Sciences, Yokohama, Kanagawa, 230-0045, Japan

40 [15] Laboratory of Immunology, Institute for Frontier Life and Medical Sciences, Kyoto
41 University, Kyoto, Kyoto, 606-8507, Japan

42 *Corresponding author. Email: aikotani@k-lab.jp

43

44 **Abstract**

Accumulated studies have reported that hematopoietic differentiation was primarily regulated by transcription factors. Early B cell factor 1 (EBF1) is an essential transcription factor for B lymphopoiesis. Contrary to the canonical notion , we found that a single miRNA, miRNA-195 (miR-195) transduction let EBF1 deficient hematopoietic progenitor cells (HPCs) express CD19, carry out V(D)J recombination and class switch recombination, which implied that B cell matured without EBF1. A part of the mechanism was caused by FOXO1 accumulation via inhibition of FOXO1 phosphorylation pathways in which targets of miR-195 are enriched. These results suggested that some miRNA transductions could function as alternatives to transcription factors.

Introduction

Developmental hierarchy in hematopoiesis has been widely researched and it is well-known that proper stimulation leads hematopoietic stem cell into B cell lineage. Lineage specification is primarily regulated at the transcriptional level, thus lineage-specific transcription factors are considered to indispensable for differentiation (*1*, *2*). B cell development requires multiple transcription factors especially EBF1, paired box 5 (Pax5), and E2A. Pax5 and E2A are critical transcription factors for early B cell development, but they cannot rescue EBF1-deficient HPCs from failure of B cell lineage commitment (*3*). Conversely, ectopic expression of EBF1 is able to rescue Pax5, E2A, and PU.1 deleted progenitor cells from B lymphopoiesis arrest and thus, EBF1 is considered more potent than the other transcription factors (*2*, *4*, *5*). As the most potent transcription factor, EBF1 is essential for pre-pro-B cell to become pro-B cell; namely, *Ebf1*$^{-/-}$ cell express B220 but is disable to express CD19 (*6*).

69 MicroRNAs (miRNAs) are small non-coding RNA containing approximately 22
70 nucleotides that regulate several target protein expressions mediating deadenylation and
71 translation by post-transcriptionally repressing or decaying target messenger RNAs
72 (mRNAs) (*7–10*). Although similar to transcription factor, miRNAs regulate large
73 numbers of target mRNAs and deeply contribute to various cell events, the regulation is
74 mainly required for negative regulation of leaky gene expression and often called as
75 fine-tuning (*11*, *12*). In hematopoiesis, miRNAs are expressed in lineage specific
76 manner and their profiles greatly influence on cell differentiation (*13–15*). Focusing on
77 B cell development, it is revealed that Dicer, a key enzyme of miRNA generation, is
78 essential for pre- to pro- B cell transition (*16*). Individual miRNA is also studied and
79 miR-150 and miR-126 are identified as relational factor to B cell lineage development.
80 miR-150 regulate B cell differentiation by controlling c-Myb expression and miR-126
81 partially rescues EBF1 deficient B cell lineage commitment by modulating IRS-1
82 expression (*17*, *18*). Both miRNAs dramatically contributed to B cell development
83 processes, but they were not able to recover B cell development from EBF1 deficiency.
84 Conceived from these vigorous functions of miRNAs on B cell development, in this
85 time, we analyzed ability of miR-195, recently revealed as an important factor for
86 several cell differentiation, on B cell lineage commitment in EBF1 deficient HPCs (*19*,
87 *20*).
88
89 **Results**
90 **miR-195 induces B cell character in EBF1 deficient HPCs**
91 To test function of miR-195 in B cell development, we analyzed the expression levels of
92 the miRNA in mouse early hematopoietic lineages mainly focused on B cells. Although

93 the expression level was not high in mature B cell, upregulated in B cell developmental
94 steps especially during early stages (Fig. 1A). This expression profile suggested the
95 possibility of miR-195 as a potential regulator in B cell lineage commitment. To assess
96 the contribution of miR-195 on B cell development, miR-195 was transduced into mouse
97 fetal liver (FL)-derived Lin$^-$ c-kit$^+$ HPCs and the cells were differentiated to B220 and
98 CD19 expressing pro-B cells with IL7, Flt ligand and SCF on OP9 stroma cells. After 7
99 days of culture, certain numbers of the cells gradually expressed CD19, and the positive
100 cells was increased by miR-195 transduction (Fig. 1B). This result suggests that miR-195
101 has ability to shift the HPCs differentiation toward B cells. Next, we attempted to
102 differentiate *Ebf1*$^{-/-}$ FL HPC to B cell with miR-195 transduction (Fig. 1C). As by a
103 previous study (*6*), control *Ebf1*$^{-/-}$ FL HPCs expressed B220 but did not express CD19.
104 However, miR-195 transduced *Ebf1*$^{-/-}$ FL HPCs highly expressed CD19 (Fig. 1D). In
105 normal B cell development, CD19 expression follows B220 expression and hence CD19
106 positive cells show B220 expression as well. Thus, miR-195 transduced *Ebf1*$^{-/-}$ FL HPCs
107 which including B220 negative CD19 positive population may simply reflect up-
108 regulation of CD19 expression, but not B cell development. To exclude this possibility,
109 gene expressions of miR-195 transduced *Ebf1*$^{-/-}$ FL HPCs by cDNA microarray assay
110 were investigated then indicated that miR-195 transduced cells more expressed B cell
111 lineage related genes, e.g., *Pax5, Aicda*, *Rag1*, *Rag2*, *CD79b* and *Runx2*, whereas less
112 expressed T cell and NK cell lineage related genes, including *Gata3, Id2*, *Lck*, *CD3e* and
113 *Il2rb* and also myeloid lineage related genes for example, *Cebpe*, *Ly6g*, *Fcgr1*, *Fcgr2b*
114 and *fcgr3* (Fig. 1E). These results suggested that not only CD19 expression but also up-
115 regulation of several B cell developmental factors and down-regulation of other lineage
116 related genes were involved in the promotion of B cell lineage commitment by miR-195.

117

118 **EBF1 deficient HPCs were able to commit B cell lineage by transduction of miR-**
119 **195 with bone marrow niche modification**

120 The ectopic miR-195 expression led *Ebf1*$^{-/-}$ HPCs induced differentiation toward B cell.
121 However, a large part of the miR-195 transduced HPCs expressed CD19 but not B220
122 that implied they strayed from the canonical B cell differentiation steps (Fig. 1D). In
123 addition to the inner state, the microenvironment known as niche was also critically
124 involved in hematopoiesis (*21*). Especially in early B cell development, bone marrow
125 niches precisely controlled the maintenance and differentiation of lineage precursors by
126 cytokines and chemokines (*22*). Then to explore the development of miR-195 transduced
127 *Ebf1*$^{-/-}$ FL HPCs under bone marrow niche, we engrafted miR-195 transduced *Ebf1*$^{-/-}$ early
128 B cells into NOG and B6RG mice, in which absence of B cell makes the engrafted B
129 cell visible (Fig. 2A). After 7 days, the engrafted cells successfully adapted in the bone
130 marrow. While there was no remarkable change in control cell population, notably,
131 instead of B220 negative CD19 positive cells, the double positive cells were markedly
132 increased in miR-195 transduced *Ebf1*$^{-/-}$ FL early B cells which suggest the normal
133 stepwise B cell development occurred (Fig.2B). In B cell development, after CD19
134 expression, most prominent steps are VDJ recombination and subsequential IgM
135 expression on cell surface. In addition to CD19 expression, EBF1 is known to also
136 essential for VDJ recombination especially V_H to DJ_H recombination (*23*). To determine
137 whether miR-195 transduced *Ebf1*$^{-/-}$ cell rearranged the VDJ region, we attempt to detect
138 V_H-J_H assembled gene segments in the engrafted mouse bone marrow cell by digital PCR.
139 The data revealed that there were certain number of V_H-J_H segments in the bone marrow
140 of mouse engrafted miR-195 transduced *Ebf1*$^{-/-}$ cells (Fig.2C). Subsequently, to expect

141 the EBF1 independent reconstitution enabled B cell receptor to express as IgM, we
142 analyzed B cell populations in the engrafted mouse bone marrow. Not much but some
143 miR-195 transduced cells expressed IgM on cell surface likely as normal immature B cell
144 in bone marrow after 10 days from engrafted (Fig.2D). Moreover, those IgM positive
145 cells were also detected in splenocytes. These data suggested that engrafted cells had
146 differentiated to IgM positive immature or mature B cells and has been recruited to spleen.
147 The critical function of B cell is changing B cell receptor from IgM to IgG following class
148 switch DNA recombination accompanied by cell proliferation by the stimuli. To clarify
149 whether miR-195 transduced *Ebf1*$^{-/-}$ B cells have the function, whole splenocyte of the
150 engrafted mouse were stimulated with IL-4 and LPS, which causes class switch
151 recombination to IgG1 (*24*). While control transduced GFP positive cells did not expand
152 by the stimuli, miR-195 transduced GFP positive cells expanded enough to be surely
153 detected and importantly a part of them expressed IgG1 (Fig.2E). These data suggested
154 that miR-195 has potential to induce B cell differentiation from HPCs to mature B cells
155 to show class swich recombination even when critical regulator EBF1 is absent.
156

157 **miR-195 physiologically maintains several B cell populations**

158 As ectopic miR-195 expression revealed its potential in B cell development. Next, to
159 investigate contribution of endogenous miR-195 for B cell lineage populations, miR-195
160 deficient mouse in which the genome around miR-195-5p was eliminated by
161 CRISPR/CAS9 system was established. The analysis of HPC lineage populations in the
162 bone marrow revealed that several B cell related progenitor were relatively reduced in
163 miR-195$^{-/-}$ mouse. Sca-1^{-} c-kit^{+} common myeloid progenitor cell population was
164 increased but controversially, Sca-1^{+} c-kit^{-} (LSK^{-}) cells was decreased in miR-195$^{-/-}$

165 mouse (Fig. 3A). As LSK$^-$ cells mainly includes early lymphoid precursor, these results
166 suggested that miR-195 is involved in hematopoiesis including differentiation of stem
167 cells toward lymphoid and early B cells (*25*). While analysis of each early B cell
168 populations did not show significant difference, whole B220$^+$ IgM$^-$ pre B cell populations
169 was slightly increased in the BM of miR-195$^{-/-}$ mouse (Fig. 3B). In the splenic B cells,
170 marginal zone B (MZB) cells was reduced in miR-195$^{-/-}$ mouse (Fig. 3C). MZB cells was
171 previously reported to be highly dependent on EBF1 activity and disappear in absence of
172 EBF1. B-1 cells was likewise crucially regulated EBF1 as well(*26*). In the peritoneal
173 cavity of miR-195$^{-/-}$ mouse, B-1 cells was significantly decreased (Fig. 3D). These results
174 suggested that miR-195 contributed to maintain several EBF1 dependent mature B cell
175 populations at least in a part. Together, those results were in line with the results obtained
176 from extopic expression of miR-195.
177
178 **FOXO1 phosphorylation pathway targetted by miR-195 was responsible for B cell**
179 **lineage commitment**
180 To elucidate how miR-195 promote B cell development in EBF1 deficient HPC, we
181 analyzed regulatory networks of predicted miR-195 target genes by using starBase_v2.0
182 and David Bioinformatics Resources 6.8 in KEGG pathway database (*27–33*). Several
183 gene regulation networks were detected as candidates of responsible pathways on the
184 miR-195 function. Remarkably, MAPK signaling pathway and PI3K-Akt signaling
185 pathway included various targets of miR-195. Both MAPK and Akt were known to
186 phosphorylate and degrade FOXO1, which was a critical factor in several stages of B cell
187 development (*34*). Thereby, we focused on the predicted miR-195 targets: *Pik3r1*, *Pdpk1*,
188 *Akt3*, *Raf1*, *Sos2* and *Mapk3*, which were involved in and activate MAPK and PI3K-Akt

189 pathways. First, to confirm the predicted targets are actually regulated by miR-195, we
190 picked up 3'UTR of *Mapk3* and *Akt3* which were especially important in the pathways
191 and inserted in a luciferase reporter assay plasmid. As expected, although the luciferase
192 activity was down-regulated by miR-195 transduction, was not impaired by transduction
193 of miR-195 mutant of mature miRNA region (Fig. 4A). Furthermore, to determine
194 whether the predicted targets were actually regulated by miR-195, we measured the
195 expression levels in miR-195 transduced *Ebf1*$^{-/-}$ HPCs and qPCR analysis showed that
196 miR-195 transduction certainly decreased the mRNA levels (Fig. 4B). Next, to evaluate
197 inhibition of FOXO1 phosphorylation and degradation by miR-195, we compared protein
198 levels of FOXO1 and phosphorylated FOXO1 (pFOXO1) in miR-195 transduced *Ebf1*$^{-/-}$
199 HPCs. The western blotting results revealed that miR-195 transduction decreased
200 pFOXO1 levels and increased relative FOXO1 protein levels (Fig. 4C). Finally, to
201 determine whether FOXO1 accumulation is enough to enable *Ebf1*$^{-/-}$ HPCs to differentiate
202 into pro-B cells, *Ebf1*$^{-/-}$ HPCs were transduced *Foxo1* and cultured with the B cell
203 differentiating condition. As a result, similar to miR-195 transduction, Foxo1
204 transduction arose B220 and CD19 double positive *Ebf1*$^{-/-}$ cells accompanied with CD19
205 positive but B220 negative population (Fig. 4D). These data indicated that FOXO1
206 accumulation by inhibition of phosphorylating pathways was responsible for *Ebf1*$^{-/-}$ HPCs
207 to differentiate into B cell lineage.
208
209 **Less genes are epigenetically activated in pro-B cells by miR-195 than EBF1**
210 In B cell development, epigenetic changing of transcription factors and differentiation
211 molecules is crucial for proper development, which is mainly regulated by EBF1 (*35*, *36*).
212 We investigated transposase-accessible chromatin using sequencing (ATAC-seq) data of

213 *Ebf1*$^{-/-}$ pro-B cells and wild type pro-B cells from GSE92434 and cells in early B cell
214 lineages from GSE100738. While wild type pro-B cells/ *Ebf1*$^{-/-}$ pro-B cells differentially
215 accessible (DA) ATAC peaks were observed in 2809 sites, early B cells wild type CD19
216 positive/ CD19 negative cells DA ATAC peaks were in 904 sites . Then, 678 sites were
217 overlapped, which were considered to be regulated by EBF1 as impotant locus for early
218 B cell development. Moreover, among them, some peaks were overlapped with miR-
219 195 induced B220 and CD19 double positive *Ebf1*$^{-/-}$ cells(miR-195 CD19+) / B220
220 positive CD19 negative *Ebf1*$^{-/-}$ cells(control CD19-) DA ATAC peaks (73 out of 226
221 peaks) which were considered to be regulated by miR-195 (Fig. 5B). The 73 genes
222 included *Pax5*, *Runx1*, *Erg*, *Ifr8*, and *Blnk* which were well-known important genes for
223 early B cell development and several B cell related genes for example, *Rarres1*, *Ciita*,
224 *Atg7* (fig S1, S2). These results indicated that miR-195 opened less gene locus than EBF1
225 but several key locus for B cell differentiation were involved in them and they were
226 enough to differentiate the progenitor cells to mature B cells. Moreover, HOMER Motif
227 Analysis revealed that enriched motives opened by EBF1 and by miR-195 were 198 and
228 111, respectively (Fig. 5C). The common motives were 104 which included critical genes
229 for B cell development such as E2A, Foxo1 and PAX5 and high ranked motives were
230 very similar between EBF1 and miR-195 (Fig .5D). The results suggested that miR-195
231 transduction opened important chromatin regions for early B cells, which were normally
232 regulated by EBF1. Finally, we concluded that miR-195 transduction was able to
233 compensate EBF1 deficiency in B cell development by FOXO1 activation, and epigenetic
234 regulation of several B cell related genes.
235
236

237 **Discussion**

238 The canonical notion of hematopoietic fate determination implies that EBF1 is an
239 indispensable factor for B lymphopoiesis. However, in this study, we showed that a single
240 microRNA miR-195 rescued the arrest of pro-B cell differentiation induced by EBF1
241 deficiency. As miRNA plays roles in a bundle of their family, single miRNA deficient
242 mouse often doesn't show significant phenotype (*37*). Nevertheless, miR-195 deficient
243 mouse showed not much but sure decreased number of several hematopoietic cells
244 including marginal zone B cells and peritoneal B-1 cells which were reported to almost
245 dissappear in EBF1 ihCd2 mouse in which EBF1 was deficient in mature B cells (*38*).
246 Therefore, miR-195 considered to have similar function with EBF1 to some extent.
247 Considering that other miRNA deficient mice have subtle phenotype, and miR-195 is one
248 of the large family, miR-15/16 and miR-195/497 (*39*), the remarkable potential of miR-
249 195 is beyond a fine tuner as microRNA considered at least with regard to B cell lineage
250 commitment.

251 A part of the mechanisms of the potent function of miR-195 was caused by inhibition of
252 phosphorylation of FOXO1. FOXO1 is a transcriptional factor controlled by EBF1 and
253 strongly promote differentiation of pre-B cell. FOXO1 activity is regulated by
254 PI3K/AKT pathway and several miRNAs were reported to be involved in the regulation
255 (*40*). We showed *Foxo1* transduction enable EBF1 deficient cell to express CD19.
256 However, the CD19 positive cells were rapidly disappeared and couldn't be detected in
257 transplanted mouse (data not shown). It is presumable that FOXO1 activity was
258 necessary to express CD19, but other factors undertake maintenance and proliferation of
259 the developing cells. ATAC-seq analysis revealed that miR-195 was directly or

260 indirectly, involved in chromatin accessibility. As the chromatin regions and motives
261 opened by miR-195 were critical for B cell differentiation and hematopoiesis, further
262 investigation is needed for the mechanism.

263 **Materials and Methods**

264 **Plasmid construction**

265 To construct MDH1-PGK-GFP-miR-195, genomic DNA was first extracted from
266 RS4;11 using the DNeasy Tissue Extraction Kit (Qiagen). Next, a segment around miR-
267 195 was amplified by means of PCR, using Pfx polymerase (Invitrogen) and the
268 oligonucleotides, 5′ -AGATCTCTCGAGAAGGAGAGGGTGGGGTAT-3′ and 5′ -
269 GGGGCGGAATTCGCTATTCCCGCATAAGCA-3′. The obtained PCR product was
270 then cloned into the XhoI-EcoRI site of MDH1-PGK-GFP 2.0 (Addgene #11375). To
271 construct pMYs-RFP-Foxo1, first, pEX-Foxo1 (in which mouse Foxo1 is optimized for
272 gene synthesis; Eurofins Genomics K.K.) was synthesized and inserted into the EcoRI-
273 XhoI site of pEX. Next, the Foxo1 region was extracted using the restriction enzymes
274 and inserted into pMYs-RFP retroviral vector (kindly provided by Prof. T. Kitamura,
275 Tokyo University). For in vitro transcription of small-guide RNA (sgRNA), pUC57-
276 195sg-upstream and -downstream were generated. Both plasmids originated from the
277 pUC57-sgRNA expression vector (Addgene #51132), and the annealed oligonucleotides
278 were inserted into a BsaI site (For the former, 5′ -
279 TAGGCCCACAAAGGCAGGGACCTA-3′ and 5′ -
280 AAACTAGGTCCCTGCCTTTGTGGG-3′ were annealed, while for the latter, 5′ -
281 TAGGGGAAGTGAGTCTGCCAATAT-3′ and 5′ -
282 AAACATATTGGCAGACTCACTTCC-3′ were annealed). For the Dual-Luciferase®

283 assay, psiCHECK-2 vector was purchased from Promega and the 3′ -UTRs of Akt3 and
284 Mapk3 were inserted between the XhoI and NotI sites. MDH1-PGK-GFP-miR-195-mut
285 was generated by mutating 6 bases, from the second to seventh bases of the mature
286 miR-195 and complimentary regions of the stem loop structure in MDH1-PGK-GFP-
287 miR-195. In detail, normal miR-195 stem loop sequence 5′ -
288 AGCUUCCCUGGCUCUAGCAGCACAGAAAUAUUGGCACAGGGAAGCGAGUC
289 UGCCAAUAUUGGCUGUGCUGCUCCAGGCAGGGUGGUG-3′ (mature miR-195-
290 5p sequence 5′ -UAGCAGCACAGAAAUAUUGGC-3′) was mutated to 5′ -
291 AGCUUCCCUGGCUCUgcgccgACAGAAAUAUUGGCACAGGGAAGCGAGUCU
292 GCCAAUAUUGGCUGUcggcgcCCAGGCAGGGUGGUG-3′ (mature sequence 5′ -
293 UgcgccgACAGAAAUAUUGGC-3′).

294 **Animals**

295 C57BL/6 mice were purchased from CLEA Japan Inc. NOD/Shi-scid,IL-2RγKO (NOG)
296 and B6RG mice were purchased from Central Institute for Experimental Animals
297 (CIEA) . The Ebf1$^{-/+}$ mouse was originally generated by R. Grosschedl (39). miR-195-
298 deficient mice were generated based on the CRISPR/Cas9 system established by C.
299 Gurumurthy (40), using pUC57-195sg-upstream and -downstream for sgRNA
300 expression and pBGK (Addgene #65796) for Cas9 mRNA expression. The obtained
301 mice were subsequently bred and housed at Tokai University. All the animal
302 experiments in this study complied with the Guidelines for the Care and Use of Animals
303 for Scientific Purposes at Tokai University. To reduce the number of sacrificed animals,
304 the sample sizes for each animal experiment were empirically determined from previous
305 studies or the results of the first littermate mice.

306 **Flow cytometry analysis**

307 Cells were collected and washed in FACS buffer (phosphate-buffered saline
308 supplemented with 2% fetal bovine serum) and subsequently stained with the following
309 antibodies purchased from BioLegend : anti-c-kit (2B8), -Sca-1 (D7), -IL7Rα (A7R34),
310 -B220 (RA3-6B2), -IgM (RMM-1), -CD3ε (145-2C11), -CD4 (GK1.5), -CD8 (53-6.7),
311 -CD11b (M1/70), -CD19 (1D3), -CD23 (B3B4), and -IgG1 (RMG1-1) and Thermo
312 Fisher : anti-Flt3 (A2F10), -CD43 (eBioR2/60), and -CD21/35 (eBio8D9). All samples
313 were analyzed on the BD FACSVerse™ system and the data obtained was analyzed
314 using FlowJo. FACSAria™ III was used for cell sorting.

315 **Culture of lineage-negative (Lin^{-}) cells from the fetal liver**

316 Fetal livers were harvested from pregnant C57BL/6 or *Ebf1*$^{+/-}$ mice (mated with
317 *Ebf1*$^{+/-}$ male) at 13.5 days after vaginal plug formation and minced gently by means of
318 pipetting. The cell suspensions were filtered through a 67-µm pore nylon mesh and Lin^{-}
319 cells were collected using the Lineage Cell Depletion Kit, mouse and AutoMACS® Pro
320 Separator (Miltenyi Biotec), according to the manufacturer's instructions. Subsequently,
321 the collected Lin^{-} cells were transduced with miR-195 or *Foxo1* by means of retroviral
322 transfection. In brief, Platinum-E cells were transfected with MDH1-PGK-GFP (for
323 EMPTY sample) or MDH1-PGK-GFP-miR-195 or pMYs-RFP-Foxo1 using PEI
324 MAX® (Polysciences Inc.), and retroviral supernatants were harvested 48 hours later.
325 Lin^{-} cells were infected with the supernatants using 10 µg/mL Polybrene (Sigma-
326 Aldrich). The infected and transduced Lin^{-} cells were cultured and differentiated into B
327 cells on OP9 cells in IMDM (Thermo Fisher) supplemented with 10% fetal bovine
328 serum, 1 mM sodium pyruvate, 0.1 mM non-essential amino acid solution, 50 µM 2-
329 mercaptoethanol, 100 units/mL penicillin G, 100 µg/mL streptomycin (all from Wako),
330 and 10 ng/mL recombinant SCF, IL-7, and Flt3-ligand (R&D Systems). For *in vivo*

331 analysis of B cell development of EBF1$^{-/-}$ Lin^{-} cells, 1×10^{6} cells were injected into the
332 NOG or B6RG mice after >7 days of culture and expanded *in vitro*.

333 **Microarray analysis**

334 Total RNA was isolated using the RNeasy MINI Kit (Qiagen), and its quality was
335 analyzed using the 2100 Bioanalyzer (Agilent Technologies). Approximately 100 ng
336 RNA was labeled, and gene expression microarray analysis was performed using the
337 Agilent Whole Mouse Genome Microarray 4x44K v2 (Agilent Technologies),
338 according to the manufacturer's instructions. The processed data was analyzed using
339 GeneSpring GX version 14.9 (Agilent Technologies). Raw intensity values were
340 normalized using the 75th percentile and transformed to the Log_2 scale. All experiments
341 were carried out in duplicates.

342 **Droplet digital PCR (ddPCR)**

343 To carry out ddPCR for VJ recombination analysis, total DNA was isolated from whole
344 cells of the bone marrow in miR-195-transduced *Ebf1*$^{-/-}$ FL HPCs-engrafted NOG mice,
345 using the Wizard® Genomic DNA Purification Kit (Promega). ddPCR was conducted
346 using QX100 Droplet Digital PCR system (Bio-Rad). Briefly, 3.3 μL of template cDNA
347 with 20× primer and a TaqMan™ probe set was partitioned into approximately 20,000
348 droplets using the QX100 Droplet Generator, for amplification. The cycling conditions
349 were 95°C for 10 min, followed by 50 cycles of 95°C for 15 sec and 60°C for 1 min,
350 and a final 10-min incubation at 98°C. The droplets were subsequently read
351 automatically using the QX10 droplet reader. The data were analyzed with QuantaSoft
352 analysis software (ver. 1.3.2.0; Bio-Rad). The primers used were as follows: forward
353 primer – 5′-GAGGACTCTGCRGTCTATTWCTGTGC-3′; reverse primer – 5′-

354 CCCTGACCCAGACCCATGT-3′; and probe – 5′-6FAM-

355 TTCAACCCCTTTGTCCCAAAGTT-TAM-3′.

356 **Class-switch stimulation**

357 EBF1$^{-/-}$ Lin^{-} cells were transduced with EMPTY and miR-195-expressing vector and

358 transplanted into B6RG mice. At 10 days post-transplantation, the spleens were

359 collected from the mice, minced with slide glasses, and filtered through a 67-µm pore

360 nylon mesh. IgM^{+} cells were sorted and stimulated for 3 days with 12.5 µg/mL

361 lipopolysaccharide (Sigma-Aldrich) and 7.5 ng/mL IL-4 (Peprotech) in RPMI-1640

362 (Wako) supplemented with 10% fetal bovine serum, 100 U/mL penicillin G, and 100

363 µg/mL streptomycin.

364 **Gene Ontology analysis**

365 The miR-195 targetomes were gathered from the miR-195 target mRNAs identified

366 from three databases (Targetscan, miRDB, and microRNA.org) and by comparing the

367 microarray data of the targets in control- and miR-195-transduced Ebf1$^{-/-}$ FL HPCs. To

368 investigate the biological functions, these genes were applied to the Gene Ontology

369 classification using GeneSpringGX11.

370 **Quantitative real-time PCR**

371 For mRNA quantification, total RNA was isolated using Sepasol-RNA I Super G

372 (Nacalai Tesque) and cDNA was synthesized from it using the ReverTra Ace™ qPCR

373 RT Master Mix (TOYOBO). qPCR was performed using THUNDERBIRD™ SYBR®

374 qPCR Mix (TOYOBO) on the StepOnePlus™ Real-Time PCR System (Thermo

375 Fisher). The following primers were used for qPCR: Pik3r1 – 5′-

376 AAACTCCGAGACACTGCTGA-3′ and 5′-GAGTGTAATCGCCGTGCATT-3′;

377 Pdpk1 – 5′-CTGGGCTCTGCTCTAGTGTT-3′ and 5′-

378 CCCAGGTTCAGGACAGGATT-3′; Akt3 – 5′-
379 GTGGACCACTGTTATAGAGAGAACAT-3′ and 5′-
380 TTGGATAGCTTCCGTCCACT-3′; Raf1 – 5′-TCTTCCATCGAGCTGCTTCA-3′ and
381 5′-GGATGTAGTCAGCGTGCAAG-3′; Sos2 – 5′-AACTTTGAAGAACGGGTGGC-3′
382 and 5′-TTTCCTGCAGTGCCTCAAAC-3′; and Mapk3 – 5′-
383 ACTACCTGGACCAGCTCAAC-3′ and 5′-TAGGAAAGAGCTTGGCCCAA-3′. For
384 miR-195 quantification, TaqMan™ MicroRNA Assay (ABI) was used. Briefly, total
385 RNA was isolated using Sepasol-RNA I Super G and cDNA was synthesized from it
386 using the microRNA TaqMan™ MicroRNA Reverse Transcription Kit (Thermo Fisher)
387 and a specific primer, 5′-UAGCAGCACAGAAAUAUUGGC-3′. The expression levels
388 were measured using the TaqMan™ Fast Advanced Master Mix (Thermo Fisher) on the
389 StepOnePlus™ Real-Time PCR System. All reagents and kits in this section were used
390 according to the manufacturer's instructions. Target RNA expression levels were
391 compared with those of GAPDH using the $2^{-\Delta\Delta Ct}$ method.

392 **Dual-Luciferase® assay**

393 293T cells were co-transfected with 20 ng psiCHECK-2 of *Akt3* or *Mapk3* and 100 ng
394 MDH1-PGK-GFP-miR-195 or MDH1-PGK-GFP-miR-195-mut. At 48 hrs post-
395 transfection, the relative amounts of Renilla and firefly luciferase were analyzed using a
396 Dual-Luciferase® Reporter Assay System (Promega). The Renilla/firefly luciferase ratio
397 was calculated and normalized against the control.

398 **Western blot**

399 Total proteins were collected from whole cells using radioimmunoprecipitation assay
400 buffer (Wako) with protease inhibitor cocktail (Sigma-Aldrich) and SDS sample buffer
401 (60 mM Tris-HCl pH 6.8, 2% SDS, 10% glycerol, and 50 mM dithiothreitol). The

402 proteins were separated using SDS-PAGE and the western blot signal was detected and
403 analyzed using the Immobilon Western Chemiluminescent HRP Substrate (Millipore)
404 on Ez-Capture MG AE-9300 (ATTO). The following antibodies were used: anti-
405 FOXO1 (C29H4, Cell Signaling Technology), -phospho-FOXO1(Ser256) (9461, Cell
406 Signaling Technology), and -GAPDH (G9545, Sigma-Aldrich).

407 **ATAC-seq analysis**

408 For ATAC-seq analysis, $B220^+$ $CD19^+$ and $B220^+$ cells were sorted from the bone
409 marrow of NOG mice transplanted with miR-195-transduced $EBF1^{-/-}$ Lin^- cells. $B220^+$
410 cells were also sorted from the empty transduced sample. The collected cells were
411 resolved using CELLBANKER® (Takara Bio) and temporarily preserved at –20°C.
412 ATAC-seq libraries were prepared from the cryopreserved cells according to the Omni-
413 ATAC protocol (*41*). Briefly, >5,000 cells were lysed and subjected to a transposition
414 reaction. The transposed fragments were pre-amplified, quantitated using RT-PCR, and
415 then amplified again. The prepared libraries were sequenced on the NextSeq 550
416 platform (Illumina) with paired-end reads (read 1, 75 bp; index 1, 8 bp; index 2, 8 bp;
417 read 2, 75 bp). Short-read data were trimmed using sickle 1.33
418 (https://github.com/najoshi/sickle) and mapped onto a mm10 reference genome using
419 bowtie2. Unmapped, multi, chrM mapping, and duplicate reads were eliminated using
420 samtools 1.16.1 and Picard Tools (Picard MarkDuplicates;
421 http://broadinstitute.github.io/picard). Peak summits in all populations were determined
422 using the MACS3 functions (-callpeak -p 1e-5 https://github.com/macs3-
423 project/MACS). Motif enrichment analysis was carried out using HOMER, with default
424 settings.

425 **Statistical analysis**

426 Student's *t*-test was used to analyze differences between groups, and *p*-values<0.05
427 were considered statistically significant. All analyses were performed using Excel
428 (Microsoft). Statistical significance was determined using the Fisher's exact test,
429 followed by multiple test corrections using the Benjamini and Yekutieli false discovery
430 rate method.
431

432 **Acknowledgments**
433 We thank N. Kurosaki, K. Takahashi, E. Nagashima, and members of the Department of
434 Innovative Medical Science at Tokai University for their assistance, advice, and helpful
435 discussions. We also thank the Support Center for Medical Research and Education at
436 Tokai University for their technical assistance.
437 **Funding:**
438 This work was supported by Grants-in-Aid for Scientific Research JP20H03716 (to A.K.)
439 and JP20K17362 (to Y.M.) from the Japan Society for the Promotion of Science; P-
440 PROMOTE 22ama221213 and 22ama221215 (to A.K.) from the Japan Agency for
441 Medical Research and Development; and JST-CREST JPMJCR19H5 (to A.K.) from the
442 Japan Science and Technology Agency.
443 **Author contributions:**
444 A.K. designed the research; Y.M., R.Y., R.K., K.K., R.-K.N., and K.O. performed the
445 research; T.I., K. Hirano, H.H., K. Hozumi, M. Ohtsuka, T. Kishikawa, C.S., M. Otsuka,
446 R.M., K.A., and T. Kurosaki contributed new reagents and analytic tools; H.K. analyzed
447 the data; Y.M. and A.K. wrote the paper.
448 **Competing interests:**
449 The authors declare that they have no conflict of interest.

450 **Data and materials availability:**

451 The microarray data was deposited in Gene Expression Omnibus with the identifier
452 GSE246669, and the ATAC-seq data was also deposited with the identifier GSE246530. The
453 other data generated in this study are available in the manuscript or supplementary materials.

454

455 **References**

456 1. J. Zhu, S. G. Emerson, Hematopoietic cytokines, transcription factors and lineage
457 commitment. *Oncogene* **21**, 3295–3313 (2002).

458 2. T. Ikawa, H. Kawamoto, L. Y. T. Wright, C. Murre, Long-Term Cultured E2A-
459 Deficient Hematopoietic Progenitor Cells Are Pluripotent. *Immunity* **20**, 349–360
460 (2004).

461 3. Y. C. Lin, S. Jhunjhunwala, C. Benner, S. Heinz, E. Welinder, R. Mansson, M.
462 Sigvardsson, J. Hagman, C. A. Espinoza, J. Dutkowski, T. Ideker, C. K. Glass, C.
463 Murre, A global network of transcription factors, involving E2A, EBF1 and
464 Foxo1, that orchestrates B cell fate. *Nature Immunology* **11**, 635–643 (2010).

465 4. J. M. R. Pongubala, D. L. Northrup, D. W. Lancki, K. L. Medina, T. Treiber, E.
466 Bertolino, M. Thomas, R. Grosschedl, D. Allman, H. Singh, Transcription factor
467 EBF restricts alternative lineage options and promotes B cell fate commitment
468 independently of Pax5. *Nature Immunology* **9**, 203–215 (2008).

469 5. I. Györy, S. Boller, R. Nechanitzky, E. Mandel, S. Pott, E. Liu, R. Grosschedl,
470 Transcription factor Ebf1 regulates differentiation stage-specific signaling,
471 proliferation, and survival of B cells. *Genes Dev.* **26**, 668–682 (2012).

472 6. K. L. Medina, J. M. R. Pongubala, K. L. Reddy, D. W. Lancki, R. DeKoter, M.
473 Kieslinger, R. Grosschedl, H. Singh, Assembling a Gene Regulatory Network for
474 Specification of the B Cell Fate. *Developmental Cell* **7**, 607–617 (2004).

475 7. D. P. Bartel, MicroRNAs: Target Recognition and Regulatory Functions. *Cell* **136**,
476 215–233 (2009).

477 8. R. W. Carthew, E. J. Sontheimer, Origins and Mechanisms of miRNAs and
478 siRNAs. *Cell* **136**, 642–655 (2009).

479 9. D. Cifuentes, H. Xue, D. W. Taylor, H. Patnode, Y. Mishima, S. Cheloufi, E. Ma,
480 S. Mane, G. J. Hannon, N. D. Lawson, S. A. Wolfe, A. J. Giraldez, A Novel
481 miRNA Processing Pathway Independent of Dicer Requires Argonaute2 Catalytic
482 Activity. *Science* **328**, 1694–1698 (2010).

483 10. N. Yamakawa, K. Okuyama, J. Ogata, A. Kanai, A. Helwak, M. Takamatsu, K.
484 Imadome, K. Takakura, B. Chanda, N. Kurosaki, H. Yamamoto, K. Ando, H.
485 Matsui, T. Inaba, A. Kotani, Novel functional small RNAs are selectively loaded
486 onto mammalian Ago1. *Nucleic Acids Res* **42**, 5289–5301 (2014).

487 11. C. Sevignani, G. A. Calin, L. D. Siracusa, C. M. Croce, Mammalian microRNAs: a
488 small world for fine-tuning gene expression. *Mamm Genome* **17**, 189–202 (2006).

489 12. M. Listowski, E. Heger, D. Bogusławska, B. Machnicka, K. Kuliczkowski, J.
490 Leluk, A. Sikorski, microRNAs: fine tuning of erythropoiesis. *Cellular and*
491 *Molecular Biology Letters* **18**, 34–46 (2013).

492 13. S. Monticelli, K. M. Ansel, C. Xiao, N. D. Socci, A. M. Krichevsky, T.-H. Thai,
493 N. Rajewsky, D. S. Marks, C. Sander, K. Rajewsky, A. Rao, K. S. Kosik,
494 MicroRNA profiling of the murine hematopoietic system. *Genome Biology* **6**, R71
495 (2005).

496 14. J. R. Neilson, G. X. Y. Zheng, C. B. Burge, P. A. Sharp, Dynamic regulation of
497 miRNA expression in ordered stages of cellular development. *Genes Dev.* **21**, 578–
498 589 (2007).

499 15. C.-Z. Chen, L. Li, H. F. Lodish, D. P. Bartel, MicroRNAs Modulate
500 Hematopoietic Lineage Differentiation. *Science* **303**, 83–86 (2004).

501 16. S. B. Koralov, S. A. Muljo, G. R. Galler, A. Krek, T. Chakraborty, C.
502 Kanellopoulou, K. Jensen, B. S. Cobb, M. Merkenschlager, N. Rajewsky, K.
503 Rajewsky, Dicer Ablation Affects Antibody Diversity and Cell Survival in the B
504 Lymphocyte Lineage. *Cell* **132**, 860–874 (2008).

505 17. C. Xiao, D. P. Calado, G. Galler, T.-H. Thai, H. C. Patterson, J. Wang, N.
506 Rajewsky, T. P. Bender, K. Rajewsky, MiR-150 Controls B Cell Differentiation by
507 Targeting the Transcription Factor c-Myb. *Cell* **131**, 146–159 (2007).

508 18. K. Okuyama, T. Ikawa, B. Gentner, K. Hozumi, R. Harnprasopwat, J. Lu, R.
509 Yamashita, D. Ha, T. Toyoshima, B. Chanda, T. Kawamata, K. Yokoyama, S.
510 Wang, K. Ando, H. F. Lodish, A. Tojo, H. Kawamoto, A. Kotani, MicroRNA-
511 126–mediated control of cell fate in B-cell myeloid progenitors as a potential
512 alternative to transcriptional factors. *PNAS* **110**, 13410–13415 (2013).

513 19. H. Qiu, J. Zhong, L. Luo, Z. Tang, N. Liu, K. Kang, L. Li, D. Gou, Regulatory
514 Axis of miR-195/497 and HMGA1-Id3 Governs Muscle Cell Proliferation and
515 Differentiation. *International Journal of Biological Sciences* **13**, 157–166 (2017).

516 20. A. Dueñas, A. Expósito, M. del M. Muñoz, M. J. de Manuel, A. Cámara-Morales,
517 F. Serrano-Osorio, C. García-Padilla, F. Hernández-Torres, J. N. Domínguez, A.
518 Aránega, D. Franco, MiR-195 enhances cardiomyogenic differentiation of the
519 proepicardium/septum transversum by Smurf1 and Foxp1 modulation. *Sci Rep* **10**,
520 9334 (2020).

521 21. A. C. Gomes, T. Hara, V. Y. Lim, D. Herndler-Brandstetter, E. Nevius, T.
522 Sugiyama, S. Tani-ichi, S. Schlenner, E. Richie, H.-R. Rodewald, R. A. Flavell, T.
523 Nagasawa, K. Ikuta, J. P. Pereira, Hematopoietic Stem Cell Niches Produce
524 Lineage-Instructive Signals to Control Multipotent Progenitor Differentiation.
525 *Immunity* **45**, 1219–1231 (2016).

526 22. K. Tokoyoda, T. Egawa, T. Sugiyama, B.-I. Choi, T. Nagasawa, Cellular Niches
527 Controlling B Lymphocyte Behavior within Bone Marrow during Development.
528 *Immunity* **20**, 707–718 (2004).

529 23. J. M. R. Pongubala, D. L. Northrup, D. W. Lancki, K. L. Medina, T. Treiber, E.
530 Bertolino, M. Thomas, R. Grosschedl, D. Allman, H. Singh, Transcription factor
531 EBF restricts alternative lineage options and promotes B cell fate commitment
532 independently of Pax5. *Nat Immunol* **9**, 203–215 (2008).

533 24. M. Muramatsu, V. S. Sankaranand, S. Anant, M. Sugai, K. Kinoshita, N. O.
534 Davidson, T. Honjo, Specific Expression of Activation-induced Cytidine
535 Deaminase (AID), a Novel Member of the RNA-editing Deaminase Family in
536 Germinal Center B Cells*. *Journal of Biological Chemistry* **274**, 18470–18476
537 (1999).

538 25. R. Kumar, V. Fossati, M. Israel, H.-W. Snoeck, Lin−Sca1+Kit− Bone Marrow
539 Cells Contain Early Lymphoid-Committed Precursors That Are Distinct from
540 Common Lymphoid Progenitors. *The Journal of Immunology* **181**, 7507–7513
541 (2008).

542 26. B. Vilagos, M. Hoffmann, A. Souabni, Q. Sun, B. Werner, J. Medvedovic, I. Bilic,
543 M. Minnich, E. Axelsson, M. Jaritz, M. Busslinger, Essential role of EBF1 in the
544 generation and function of distinct mature B cell types. *Journal of Experimental*
545 *Medicine* **209**, 775–792 (2012).

546 27. J.-H. Yang, J.-H. Li, P. Shao, H. Zhou, Y.-Q. Chen, L.-H. Qu, starBase: a database
547 for exploring microRNA–mRNA interaction maps from Argonaute CLIP-Seq and
548 Degradome-Seq data. *Nucleic Acids Res* **39**, D202–D209 (2011).

549 28. J.-H. Li, S. Liu, H. Zhou, L.-H. Qu, J.-H. Yang, starBase v2.0: decoding miRNA-
550 ceRNA, miRNA-ncRNA and protein–RNA interaction networks from large-scale
551 CLIP-Seq data. *Nucleic Acids Res* **42**, D92–D97 (2014).

552 29. D. W. Huang, B. T. Sherman, R. A. Lempicki, Bioinformatics enrichment tools:
553 paths toward the comprehensive functional analysis of large gene lists. *Nucleic*
554 *Acids Res* **37**, 1–13 (2009).

555 30. D. W. Huang, B. T. Sherman, R. A. Lempicki, Systematic and integrative analysis
556 of large gene lists using DAVID bioinformatics resources. *Nature Protocols* **4**, 44–
557 57 (2009).

558 31. M. Kanehisa, S. Goto, KEGG: Kyoto Encyclopedia of Genes and Genomes.
559 *Nucleic Acids Res* **28**, 27–30 (2000).

560 32. M. Kanehisa, Y. Sato, M. Kawashima, M. Furumichi, M. Tanabe, KEGG as a
561 reference resource for gene and protein annotation. *Nucleic Acids Res* **44**, D457–
562 D462 (2016).

563 33. M. Kanehisa, M. Furumichi, M. Tanabe, Y. Sato, K. Morishima, KEGG: new
564 perspectives on genomes, pathways, diseases and drugs. *Nucleic Acids Res* **45**,
565 D353–D361 (2017).

566 34. H. S. Dengler, G. V. Baracho, S. A. Omori, S. Bruckner, K. C. Arden, D. H.
567 Castrillon, R. A. DePinho, R. C. Rickert, Distinct functions for the transcription
568 factor Foxo1 at various stages of B cell differentiation. *Nature Immunology* **9**,
569 1388–1398 (2008).

570 35. T. Treiber, E. M. Mandel, S. Pott, I. Györy, S. Firner, E. T. Liu, R. Grosschedl,
571 Early B Cell Factor 1 Regulates B Cell Gene Networks by Activation, Repression,
572 and Transcription- Independent Poising of Chromatin. *Immunity* **32**, 714–725
573 (2010).

574 36. H. Maier, R. Ostraat, H. Gao, S. Fields, S. A. Shinton, K. L. Medina, T. Ikawa, C.
575 Murre, H. Singh, R. R. Hardy, J. Hagman, Early B cell factor cooperates with
576 Runx1 and mediates epigenetic changes associated with mb-1 transcription. *Nature*
577 *Immunology* **5**, 1069–1077 (2004).

578 37. R. Song, P. Walentek, N. Sponer, A. Klimke, J. S. Lee, G. Dixon, R. Harland, Y.
579 Wan, P. Lishko, M. Lize, M. Kessel, L. He, miR-34/449 miRNAs are required for
580 motile ciliogenesis by repressing cp110. *Nature* **510**, 115–120 (2014).

581 38. B. Vilagos, M. Hoffmann, A. Souabni, Q. Sun, B. Werner, J. Medvedovic, I. Bilic,
582 M. Minnich, E. Axelsson, M. Jaritz, M. Busslinger, Essential role of EBF1 in the
583 generation and function of distinct mature B cell types. *Journal of Experimental*
584 *Medicine* **209**, 775–792 (2012).

585 39. K. Hutter, T. Rülicke, M. Drach, L. Andersen, A. Villunger, S. Herzog,
586 Differential roles of miR-15a/16-1 and miR-497/195 clusters in immune cell
587 development and homeostasis. *The FEBS Journal* **288**, 1533–1545 (2021).

588 40. M. Coffre, D. Benhamou, D. Rieß, L. Blumenberg, V. Snetkova, M. J. Hines, T.
589 Chakraborty, S. Bajwa, K. Jensen, M. M. W. Chong, L. Getu, G. J. Silverman, R.
590 Blelloch, D. R. Littman, D. Calado, D. Melamed, J. A. Skok, K. Rajewsky, S. B.
591 Koralov, miRNAs Are Essential for the Regulation of the PI3K/AKT/FOXO
592 Pathway and Receptor Editing during B Cell Maturation. *Cell Reports* **17**, 2271–
593 2285 (2016).

594

595 **Fig. 1. miR-195 promotes HPCs to differentiate into the pro-B cell stage without**
596 **EBF1.**
597 (A) Endogenous expression levels of miR-195 were measured by means of quantitative
598 RT-PCR. RNAs were collected from the following hematopoietic lineage cells in 8-week-
599 old C57BL/6 mice. KSL (c-kit^{+} Sca1^{+} Lin^{-}); lymphoid-primed multipotent progenitors
600 (LMPP: C-kit^{+} Sca1^{+} Lin^{-} Flt3^{+} IL7Rα^{-}); common lymphoid progenitors (CLP: CD43^{-}
601 IL7Rα^{+}); pro-B (B220^{+} CD43^{+} IgM^{-}); pre-B (B220^{+} CD43^{-} IgM^{-}); mature B (B220^{high}
602 CD43^{-} IgM^{+}); double-negative T (DN: CD3^{+} CD4^{-} CD8^{-}); common myeloid progenitor
603 (CMP: c-kit^{+} Sca1^{-} CD11b^{+}); myeloid cell (Mac1: c-kit^{-} Sca1^{-} CD11b^{+}). Data are shown
604 as mean ± S.D. (*n*=3). (B) Flow cytometry analysis of control and miR-195-expressing
605 Lin^{-} cells. HPCs from fetal livers of wild-type mice were cultured for 7 days on OP9 with
606 SCF, Flt3-ligand, and IL-7, after infection with control or miR-195 retrovirus.
607 Representative result of control (upper panel) and miR-195 (lower panel) viral infections
608 is shown (*n*=3). (C) Outline of the *in vitro* culture system of *Ebf1*$^{-/-}$ HPCs. (D) Flow
609 cytometry analysis of control and miR-195-expressing *Ebf1*$^{-/-}$ HPCs. Shown data is
610 representative of *n*=3. (E) Microarray analysis of miR-195-expressing *Ebf1*$^{-/-}$ HPCs. Log_2
611 fold-changes in the expression levels of genes related to B (left panel), T (middle-upper
612 panel), NK (middle-lower panel), and myeloid (right panel) cell lineages were classified
613 and are shown as colored columns. The analysis was carried out in duplicates.
614
615 **Fig. 2. miR-195 leads *Ebf1*-deficient HPCs to mature into B cells with bone marrow**
616 **niche assistance.**
617 (A) *In vivo* analysis of B cell development of *Ebf1*$^{-/-}$ HPCs. (B) Flow cytometry analysis
618 of control and miR-195-expressing *Ebf1*$^{-/-}$ HPCs in the bone marrow collected at 7 days

619 after transplantation. (C) Using droplet digital PCR, VJ region fragments were amplified
620 from the genomic DNA of B220^{+} cells in the bone marrow of mice transplanted with
621 control and miR-195-expressing *Ebf1*$^{-/-}$ HPCs. (D) Flow cytometry analysis of control
622 and miR-195-expressing *Ebf1*$^{-/-}$ HPCs in the bone marrow (BM) and spleen (SP), at 10
623 days after transplantation. (E) Flow cytometry analysis of class-switch recombination.
624 Splenocytes of mice transplanted with control and miR-195-expressing *Ebf1*$^{-/-}$ HPCs
625 were cultured for 72 hrs with IgG1 class-switch stimuli, LPS, and IL-4. Each flow
626 cytometric data is representative of n=3.
627
628 **Fig. 3. Several B cell populations are disturbed in the miR-195-deficient mouse.**
629 Flow cytometry data of B cell lineage populations in miR-195$^{-/-}$ and littermate WT mice.
630 Representative plots (left side) and mean ± S.D. of relative population rates in each
631 littermate WT mouse (right side) are shown. (A) Analysis of early B cell populations in
632 the bone marrow. Pre-pro-B (B220^{+} IgM^{-} CD43^{+} CD19^{-}); pro-B (B220^{+} IgM^{-} CD43^{+}
633 CD19^{+}); pre-B (B220^{+} IgM^{-} CD43^{-} CD19^{+}); n=5. (B) Analysis of hematopoietic
634 progenitor populations in the bone marrow; n=5. (C) Analysis of B cell populations in the
635 spleen. FO B (CD19^{+} IgM^{+} CD21/35$^{\text{low-middle}}$); MZ B (CD19^{+} IgM^{+} CD21/35^{high}); n=8.
636 (D) Analysis of B cell populations in the peritoneal cavity: B-1 (B220^{+} CD11b^{+}); B-2
637 (B220^{+} CD11b^{-}); n=7. Statistical significance was tested using two-tailed Student's t test.
638 *p<0.05; **p<0.01. WT, wild-type.
639
640 **Fig. 4. FOXO1 phosphorylation pathways are key targets of miR-195 for promotion**
641 **of B cell development.**

642 (A) Relative expression rate of miR-195 and predicted target genes were compared
643 between control (EMPTY) and miR-195-expressing *Ebf1*$^{-/-}$ HPCs. (B) Relative luciferase
644 inhibitory rates of miR-195 onto predicted target 3′-UTR were analyzed using Dual-
645 Luciferase® reporter assay. (C) Western blot of FOXO1 and phosphorylated FOXO1
646 (pFOXO1) in control and miR-195-expressing *Ebf1*$^{-/-}$ HPCs. Shown data is
647 representative of n=3. (D) Flow cytometry analysis of control and *Foxo1*-expressing
648 *Ebf1*$^{-/-}$ HPCs. Shown data is representative of n=3. Statical significance was tested using
649 two-tailed Student's t test. *p<0.05, n=3.
650
651 **Fig. 5. ATAC-seq analysis of *Ebf1*$^{-/-}$ CD19-positive B cells differentiated by miR-195.**
652 (A) Outline of analysis of open chromatin regions in miR-195-expressing *Ebf1*$^{-/-}$ cells.
653 (B) Venn diagram of numbers of genes in which DNA regions of open chromatin peaks
654 were detected by means of peak call analysis. The analyses were examined between
655 CD19-negative (FrA) and -positive (FrB, FrC, and FrD) stages of B cell development
656 (GSE100738; upper red circle); wild-type and *Ebf1*$^{-/-}$ pro-B cells (GSE92434; left-lower
657 blue circle); B220^{+} CD19^{-} cells of control and B220^{+} CD19^{+} positive miR-195-
658 expressing *Ebf1*$^{-/-}$ cells (right-lower green circle). (C and D) Venn diagram of numbers
659 of enriched known motifs detected using HOMER find motif analysis (C) and lists of
660 high p-value motifs, up to rank 10 (D).

Fig. 1

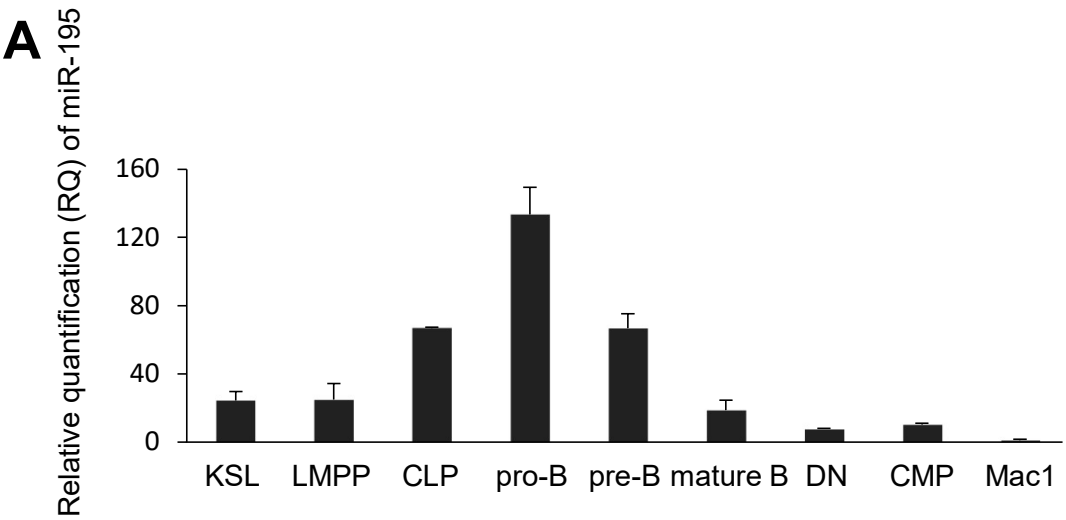
A
Relative quantification (RQ) of miR-195
160
120
80
40
0
KSL
LMPP
CLP
pro-B
pre-B
mature B
DN
CMP
Mac1

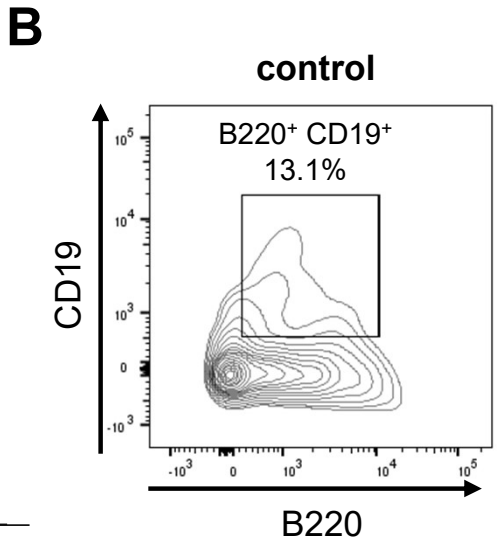
B
control
B220+ CD19+
13.1%
CD19
B220

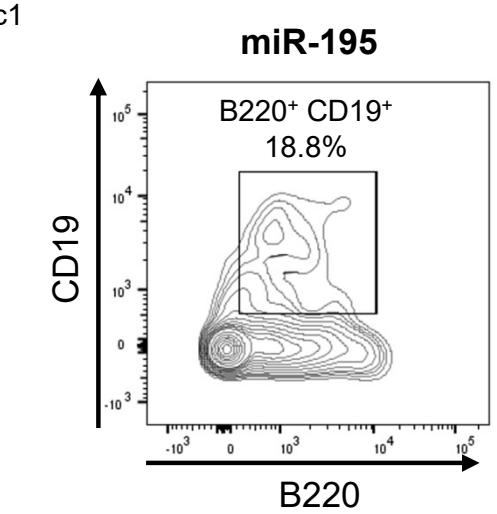
miR-195
B220+ CD19+
18.8%
CD19
B220

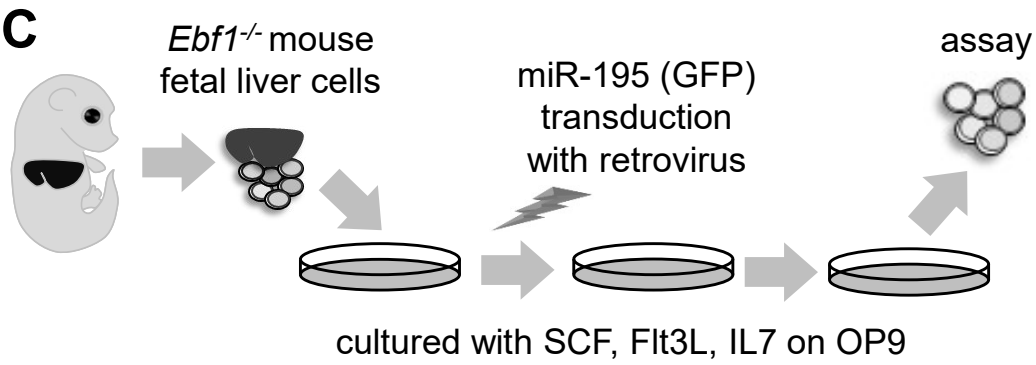
C
Ebf1-/- mouse
fetal liver cells
miR-195 (GFP)
transduction
with retrovirus
assay
cultured with SCF, Flt3L, IL7 on OP9

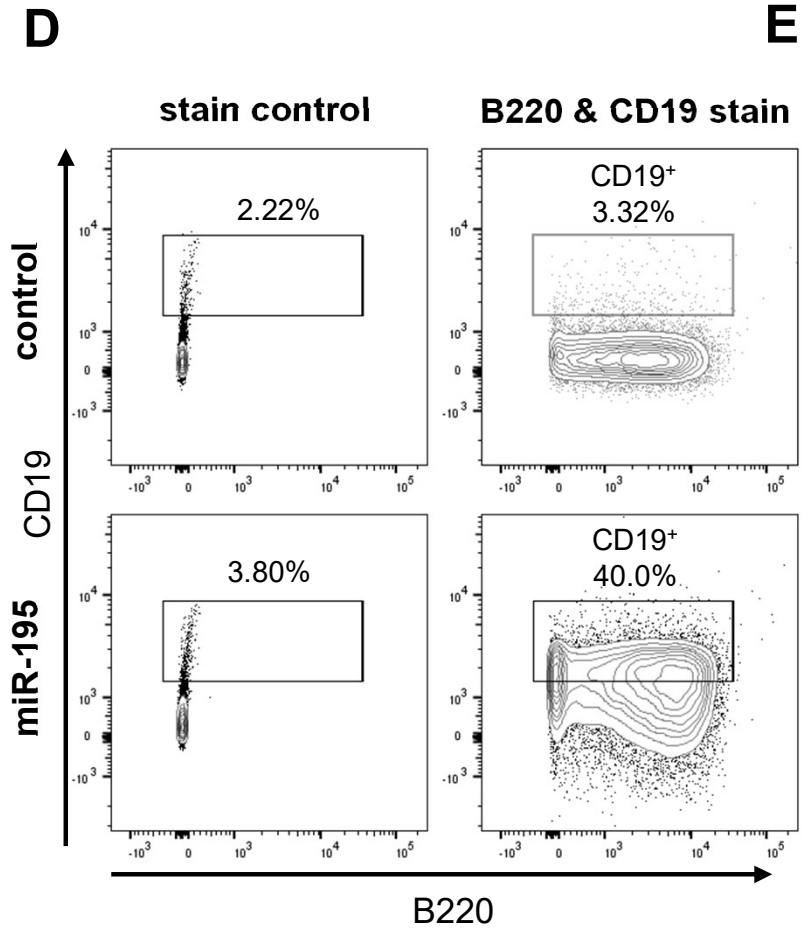
D
stain control
B220 & CD19 stain
control
miR-195
CD19
2.22%
CD19+
3.32%
3.80%
CD19+
40.0%
B220

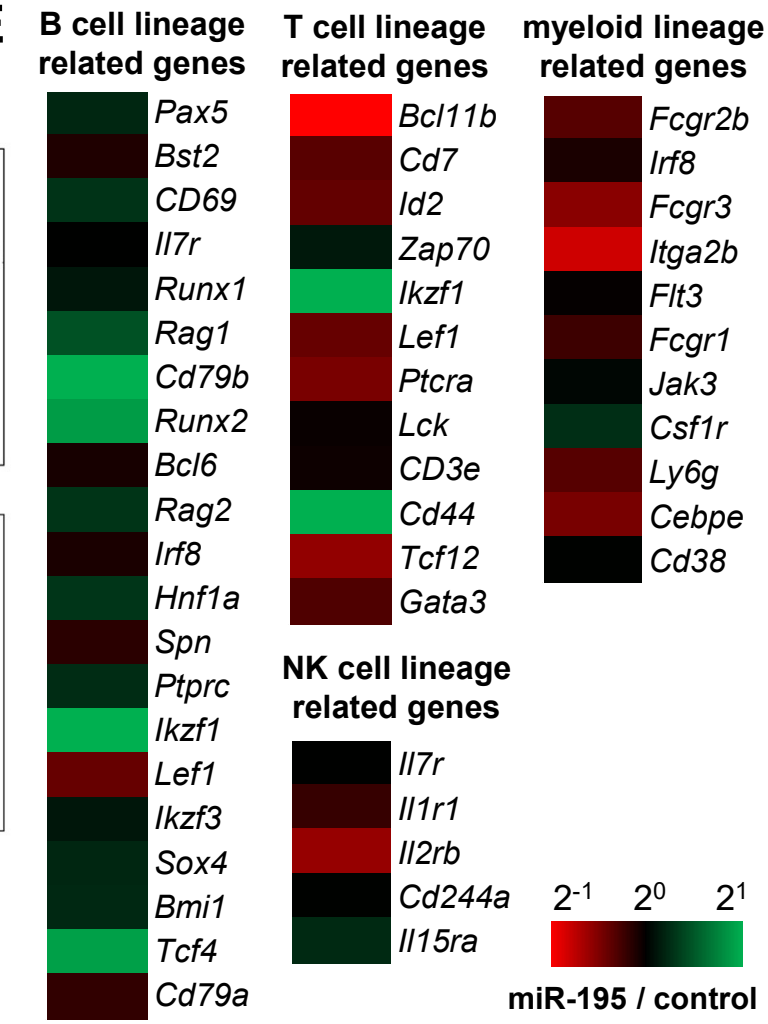
E
B cell lineage related genes
Pax5
Bst2
CD69
Il7r
Runx1
Rag1
Cd79b
Runx2
Bcl6
Rag2
Irf8
Hnf1a
Spn
Ptprc
Ikzf1
Lef1
Ikzf3
Sox4
Bmi1
Tcf4
Cd79a
T cell lineage related genes
Bcl11b
Cd7
Id2
Zap70
Ikzf1
Lef1
Ptcra
Lck
CD3e
Cd44
Tcf12
Gata3
myeloid lineage related genes
Fcgr2b
Irf8
Fcgr3
Itga2b
Flt3
Fcgr1
Jak3
Csf1r
Ly6g
Cebpe
Cd38
NK cell lineage related genes
Il7r
Il1r1
Il2rb
Cd244a
Il15ra
2-1
20
21
miR-195 / control

Fig. 2

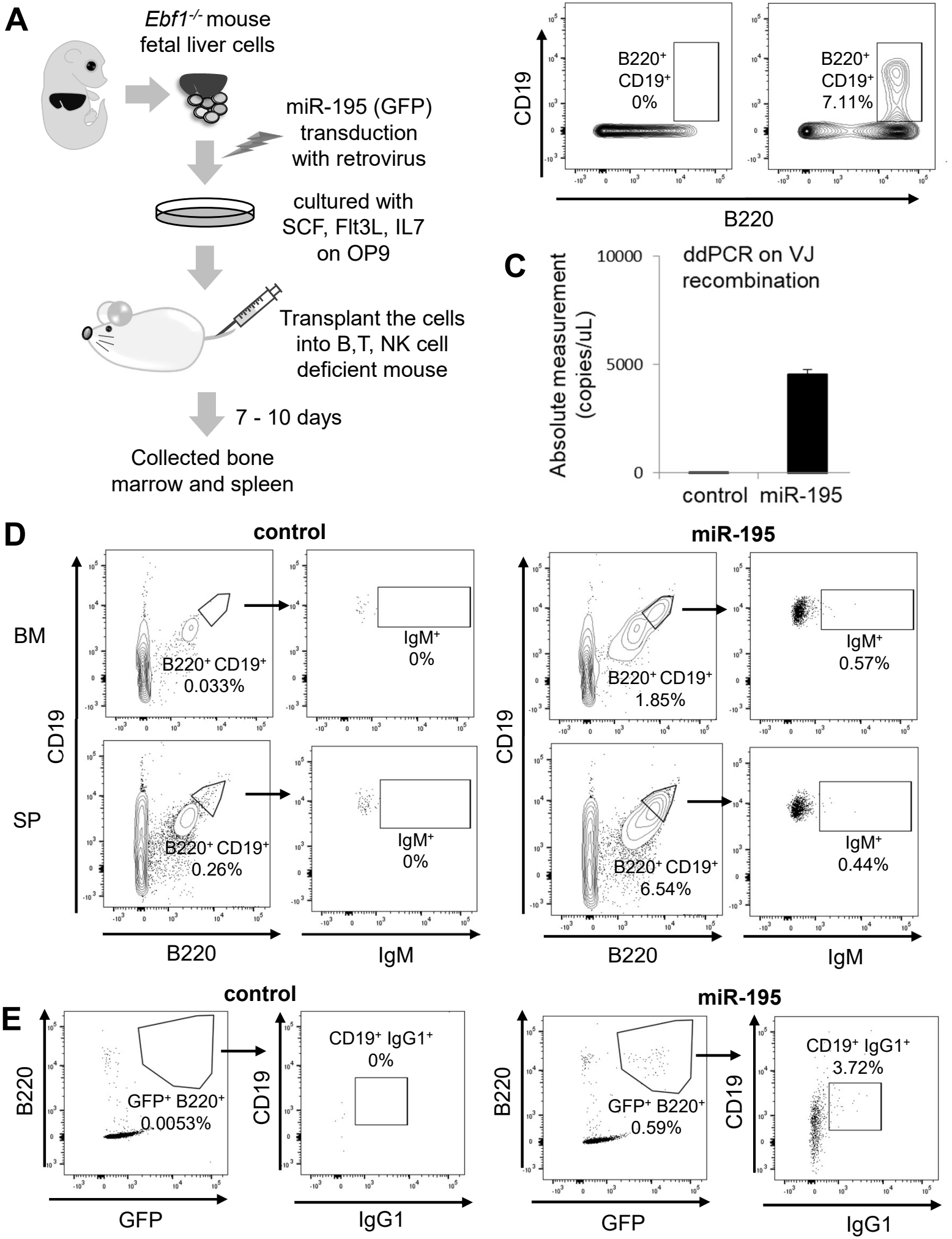
A
Ebf1-/- mouse fetal liver cells
miR-195 (GFP) transduction with retrovirus
cultured with SCF, Flt3L, IL7 on OP9
Transplant the cells into B,T, NK cell deficient mouse
7 - 10 days
Collected bone marrow and spleen
B
control
miR-195
B220+ CD19+ 0%
B220+ CD19+ 7.11%
CD19
B220
C
ddPCR on VJ recombination
Absolute measurement (copies/uL)
10000
5000
0
control
miR-195
D
control
miR-195
BM
SP
B220+ CD19+ 0.033%
IgM+ 0%
B220+ CD19+ 0.26%
IgM+ 0%
B220+ CD19+ 1.85%
IgM+ 0.57%
B220+ CD19+ 6.54%
IgM+ 0.44%
CD19
B220
IgM
E
control
miR-195
GFP+ B220+ 0.0053%
CD19+ IgG1+ 0%
GFP+ B220+ 0.59%
CD19+ IgG1+ 3.72%
B220
CD19
GFP
IgG1

Fig. 3

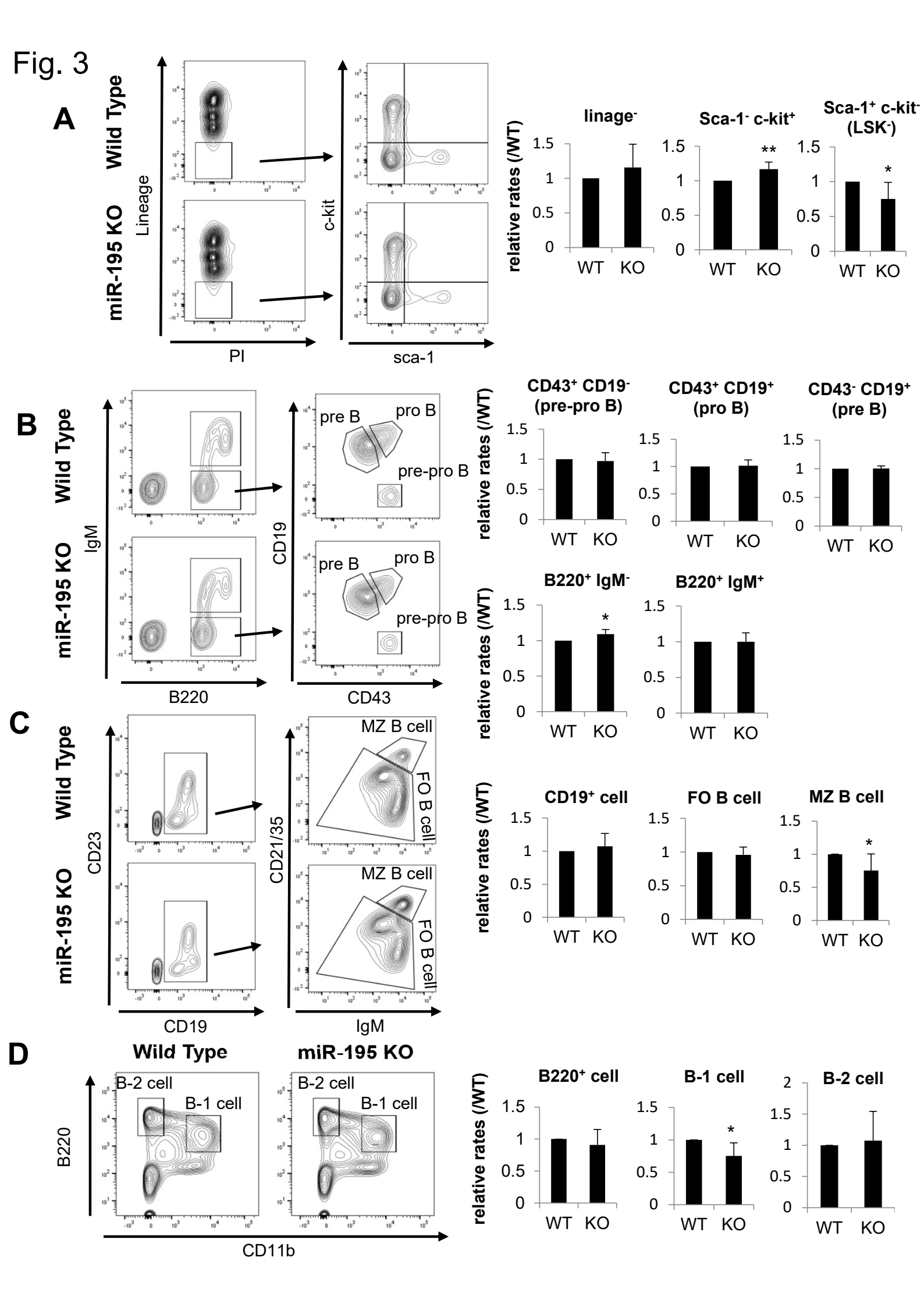
A
Wild Type
miR-195 KO
Lineage
PI
c-kit
sca-1
linage-
Sca-1- c-kit+
Sca-1+ c-kit- (LSK-)
relative rates (/WT)
WT
KO
B
IgM
B220
CD19
CD43
pre B
pro B
pre-pro B
CD43+ CD19- (pre-pro B)
CD43+ CD19+ (pro B)
CD43- CD19+ (pre B)
B220+ IgM-
B220+ IgM+
C
CD23
CD21/35
MZ B cell
FO B cell
CD19+ cell
FO B cell
MZ B cell
D
Wild Type
miR-195 KO
B-2 cell
B-1 cell
B220
CD11b
B220+ cell
B-1 cell
B-2 cell

Fig. 4

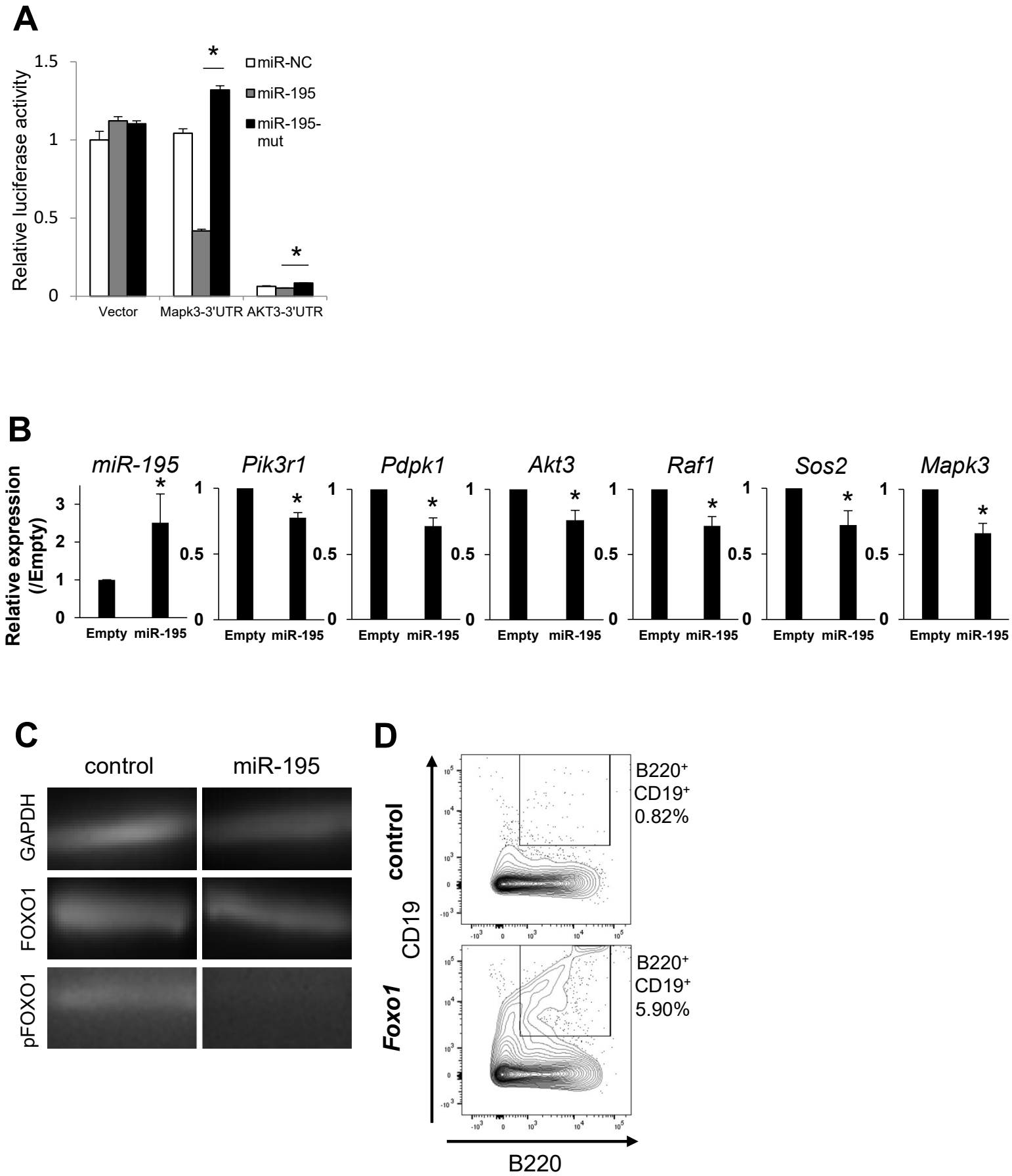
A
Relative luciferase activity
1.5
1
0.5
0
miR-NC
miR-195
miR-195-mut
*
*
Vector
Mapk3-3'UTR
AKT3-3'UTR
B
Relative expression (/Empty)
miR-195
Pik3r1
Pdpk1
Akt3
Raf1
Sos2
Mapk3
Empty
miR-195
C
control
miR-195
GAPDH
FOXO1
pFOXO1
D
control
Foxo1
CD19
B220
B220+ CD19+ 0.82%
B220+ CD19+ 5.90%

Fig. 5

A

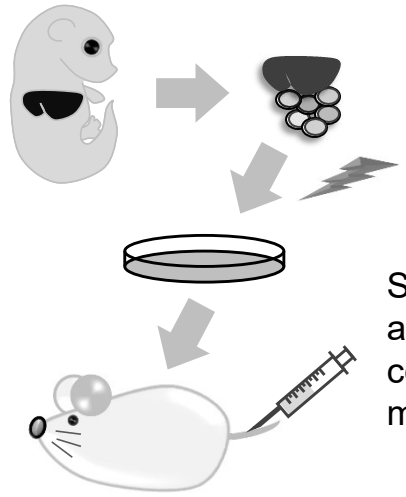

Same protocol as Fig.3A for collecting bone marrow cells

Collected B220$^+$ CD19$^+$ cells and B220$^+$ CD19$^-$ cells from bone marrow

ATAC-seq analysis

public ATAC-seq data of early B cell and EBF1 KO cells

peak call ($p<1e^{-5}$) and Enrichment motif analysis

B

numbers of genes having open chromatin peak(s)

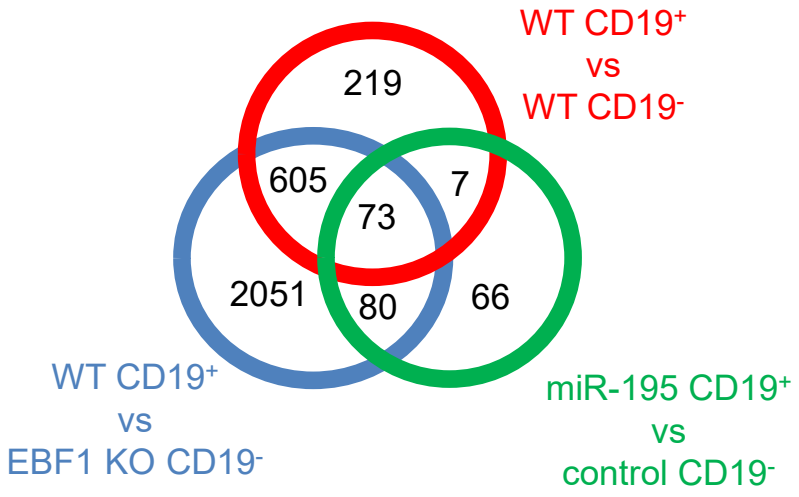

C

Enriched known motives

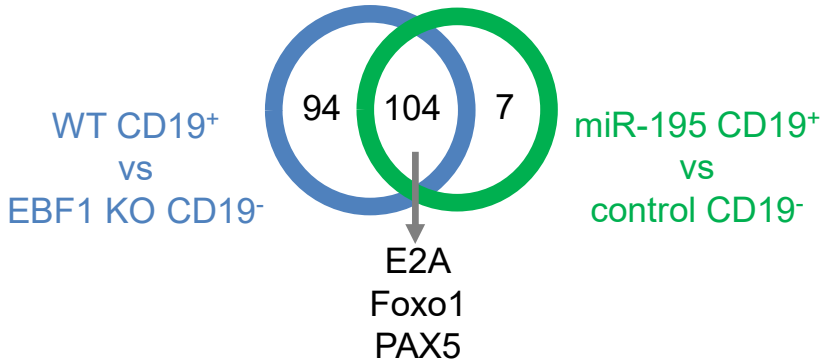

D

WT CD19$^+$ vs EBF1 KO CD19$^-$

Rank	Motif	Name	P-value
1		EBF2(EBF)/BrownAdipose-EBF2-ChIP-Seq(GSE97114)/Homer	1e-1111
2		EBF(EBF)/proBcell-EBF-ChIP-Seq(GSE21978)/Homer	1e-1047
3		Etv2(ETS)/ES-ER71-ChIP-Seq(GSE59402)/Homer	1e-810
4		ERG(ETS)/VCaP-ERG-ChIP-Seq(GSE14097)/Homer	1e-796
5		ETS1(ETS)/Jurkat-ETS1-ChIP-Seq(GSE17954)/Homer	1e-760
6		Fli1(ETS)/CD8-FLI-ChIP-Seq(GSE20898)/Homer	1e-706
7		ETV1(ETS)/GIST48-ETV1-ChIP-Seq(GSE22441)/Homer	1e-702
8		Ets1-distal(ETS)/CD4+-PolII-ChIP-Seq(Barski_et_al.)/Homer	1e-663
9		EWS:ERG-fusion(ETS)/CADO_ES1-EWS:ERG-ChIP-Seq(SRA014231)/Homer	1e-661
10		GABPA(ETS)/Jurkat-GABPa-ChIP-Seq(GSE17954)/Homer	1e-618

miR-195 CD19$^+$ vs control CD19$^-$

Rank	Motif	Name	P-value
1		Etv2(ETS)/ES-ER71-ChIP-Seq(GSE59402)/Homer	1e-55
2		ERG(ETS)/VCaP-ERG-ChIP-Seq(GSE14097)/Homer	1e-54
3		Fli1(ETS)/CD8-FLI-ChIP-Seq(GSE20898)/Homer	1e-54
4		ETV1(ETS)/GIST48-ETV1-ChIP-Seq(GSE22441)/Homer	1e-49
5		ETS1(ETS)/Jurkat-ETS1-ChIP-Seq(GSE17954)/Homer	1e-49
6		PAX5(Paired,Homeobox)/GM12878-PAX5-ChIP-Seq(GSE32465)/Homer	1e-45
7		Ets1-distal(ETS)/CD4+-PolII-ChIP-Seq(Barski_et_al.)/Homer	1e-40
8		EWS:ERG-fusion(ETS)/CADO_ES1-EWS:ERG-ChIP-Seq(SRA014231)/Homer	1e-40
9		ETV4(ETS)/HepG2-ETV4-ChIP-Seq(ENCODE)/Homer	1e-38
10		PU.1(ETS)/ThioMac-PU.1-ChIP-Seq(GSE21512)/Homer	1e-34